Six-Coordinate Thallium(III) Porphyrin Triflate: Synthesis, Physiochemical Characteristics, and X-ray Crystal Structure of (Trifluoromethanesulfonato)(tetrahydrofuran)-(*meso*-tetraphenylporphyrinato)thallium(III) Tetrahydrofuran Solvate, [Tl(tpp)(OSO_2CF_3)(THF)·THF]

Jo-Yu Tung and Jyh-Horung Chen*

Department of Chemistry, National Chung-Hsing University,
Taichung 40227, Taiwan, R.O.C

Feng-Ling Liao and Sue-Lein Wang

Department of Chemistry, National Tsing-Hua University,
Hsin-Chu 30043, Taiwan, R.O.C

Lian-Pin Hwang

Department of chemistry, National Taiwan University and
Institute of Atomic and Molecular Sciences, Academia
Sinica, Taipei 10764, Taiwan, R.O.C

Received March 23, 1998

Introduction

As widely recognized, the trifluoromethanesulfonate anion ($CF_3SO_3^-$, triflate) is an excellent leaving group in nucleophilic substitution reactions in organic chemistry.[1] Lemke *et al.*[2] investigated the ^1H, ^{19}F, and X-ray structure of bis(trifluoromethanesulfonato)(tetra-*p*-porphyrinato)silicon(IV), Si(tptp)-(OSO_2CF_3)$_2$, complex. Arnold *et al.*[3] elucidated the diaquo complex [Sn(tpp)(H_2O)$_2$](OSO_2CF_3)$_2$, indicating that the triflates were disordered in the unit cell with reasonably close O−O contacts. Goff *et al.*[4] closely examined the synthesis and ^{19}F, ^1H, and ^{13}C characterization of (trifluoromethanesulfonato)-(tetraphenylporphyrinato)iron(III), Fe(tpp)(CF_3SO_3). Guilard *et al.*[5] investigated the synthesis and ^1H characterization of (trifluoromethanesulfonato)(tetraphenylporphyrinato)gallium-(III), Ga(tpp)(CF_3SO_3), and (2,3,7,8,12,13,17,18-octaethylporphyrinato)(trifluoromethanesulfonato)gallium(III), Ga(oep)(CF_3SO_3). Although the triflate ($CF_3SO_3^-$) of Si(tptp)(CF_3SO_3)$_2$ is unidentately coordinated to the silicon atom in solid-state, according to a previous investigation, the complex Si(tptp)(CF_3SO_3)$_2$ is converted into Si(tptp)(OH)$_2$ and triflic acid (CF_3SO_2-OH) when exposed to water in a solution.[2] Similar to Si(tptp)(CF_3SO_3)$_2$, many metalloporphyrin complexes [M(por)-(CF_3SO_3)$_n$, $n = 1, 2$] do not exist for a long time outside the solid state and dissociate or react readily in a solution. Most previous studies neglect the ^{13}C and ^{19}F NMR spectra of triflate in the complexes. In this work, we largely focus on the coordination of the triflate onto the thallium porphyrin complexes. The distinction between the covalently bound CF_3SO_3 and ionic $CF_3SO_3^-$ for a novel complex (trifluoromethanesulfonato)(tetrahydrofuran)(*meso*-tetraphenylporphyrinato)thallium(III) tetrahydrofuran solvate, [Tl(tpp)(OSO_2CF_3)(THF)·THF] (**1**), in acetone-d_6 can be drawn from the ^{13}C and ^{19}F NMR spectroscopy studies of triflate ligand at 24 and −80 °C.

In light of above developments, this work synthesizes and characterizes a six-coordinate thallium(III) porphyrin complex (**1**) which appears to be the first complex with a transoid geometry. The structure of this complex and comparisons with related cisoid thallium porphyrin structures provide further insight into the area of main group porphyrin chemistry. Meanwhile, the ^{19}F and ^{13}C NMR spectra of (**1**) in a solid state at 24 °C and in acetone-d_6 at low temperature are examined to identify the bound triflate in a solid and the ionic $CF_3SO_3^-$ in solution.

Experimental Section

Preparation of [Tl(tpp)(OSO_2CF_3)(THF)·THF] (1). Tetrahydrofuran (15 mL) was added to a flask containing Tl(tpp)Cl (100 mg, 0.117 mmol) and Ag(CF_3SO_3) (60 mg, 0.234 mmol). The mixture was stirred for 2 h and then filtered through Celite. The deep red filtrate was evaporated to dryness to yield (**1**) (88.2 mg, 0.098 mmol, 84%). **1** was dissolved in THF-d_8 (99.5% from Aldrich) for ^1H NMR measurement at 24 °C. ^1H NMR, δ (ppm): 9.11 [d, β-pyrrole, ^4J(Tl−H) = 88.4 Hz], 8.26 (m, *o*-H), 7.80 (m, *m*, *p*-H). The crystals were grown from THF solution. MS, *m/z* (assignment, rel intensity): 966 ([Tl(tpp)-(SO_3CF_3)]$^+$, 11.54), 817 ([Tl(tpp)]$^+$, 100.00), 615 (H_2tpp^+, 70.57). UV/visible spectrum λ (nm) ($\epsilon \times 10^{-3}$ (M^{-1} cm^{-1})) in acetone (or THF): 332 (11.2), 410 (19.8), 430 (206.6), 530 (2.2), 564 (7.5), 604 (3.9).

Spectroscopy. Proton and ^{13}C NMR spectra in acetone-d_6 (99.96% from Aldrich) or THF-d_8 were recorded at 400.13 (or 600.20) and 100.61 (or 150.92) MHz, respectively, on Bruker AM-400 (or DMX-600) spectrometer locked on solvent deuterium, and referenced to the solvent peak. ^{19}F NMR spectra were measured in acetone-d_6 (or THF-d_8) at 282.40 MHz on Bruker MSL-300 spectrometer. Proton and ^{13}C NMR are relative to acetone-d_6 or THF-d_8 at $\delta = 2.04$ or 3.58 (the downfield resonance) and the center line of acetone-d_6 or THF-d_8 at $\delta = 29.8$ (CH_3) or 67.4 (the downfield resonance). ^{19}F data are externally relative to $CFCl_3$. Next, the temperature of the spectrometer probe was calibrated by the shift difference of methanol resonance in the ^1H NMR spectrum. The solid-state ^{13}C CP/MAS and ^{19}F MAS spectra were recorded at 24 °C at 50.33 and 470.6 MHz, respectively, on Bruker MSL-200 and Bruker MSL-500 spectrometer. In addition, dry nitrogen gas was used to drive the MAS rates of 3.7 kHz for ^{13}C and 12 kHz for ^{19}F.

The positive-ion fast atom bombardment mass spectrum (FABMS) was obtained in a nitrobenzyl alcohol (NBA) matrix using a JEOL JMS-SX/SX 102A mass spectrometer. UV/visible spectra were recorded at 24 °C on a Hitachi U-3210 spectrophotometer.

Crystallography. Table 1 presents the crystal data and other information for (**1**). X-ray structure was measured on a Siemens SMART CCD diffractometer using monochromatized Mo Kα radiation (λ = 0.710 73 Å). Absorption corrections were based on 3127 symmetry-equivalent reflections using the SHELXTL-PC program package with ($T_{\min,\max} = 0.647, 0.943$). The structures were solved by direct methods (SHELXTL PLUS) and refined by full-matrix least-squares. All non-hydrogen atoms were refined with anisotropic thermal parameters, whereas all hydrogen atom positions were calculated using a riding model and included in the structure factor calculation. Table 2 lists selected bond distances and angles.

Results and Discussion

Molecular structure of [Tl(tpp)(OSO_2CF_3)(THF)·THF] (1). Figure 1 illustrates the skeletal framework of complex **1**.

---

* To whom correspondence should be addressed.

(1) Lawrance, G. A. *Chem. Rev.* **1986**, *86*, 17.

(2) Kane, K. M.; Lemke, F. R.; Petersen, J. L. *Inorg. Chem.* **1995**, *34*, 4085.

(3) Smith, G.; Arnold, D. P.; Kennard, C. H. L.; Mak, T. C. W. *Polyhedron* **1991**, *10*, 509.

(4) Boersma A. D.; Goff, H. M. *Inorg. Chem.* **1982**, *21*, 581.

(5) Boukhris, A.; Lecomte, C.; Coutsolelos, A.; Guilard, R. *J. Organomet. Chem.* **1986**, *303*, 151.

10.1021/ic9803199 CCC: $15.00

Table 1. Crystal Data for Compound $Tl(tpp)(OSO_2CF_3)(THF)\cdot THF$ (**1**)

empirical formula	$C_{49}H_{36}F_3N_4O_4STl\cdot(C_4H_8O)$
fw	1110.4
space group	*Cc*
cryst syst	monoclinic
cryst color, habit	blue, columnar
a, Å	19.2967(1)
b, Å	11.0937(1)
c, Å	23.1386(3)
β, deg	111.702(1)
V, $Å^3$	4602(1)
Z	4
D_{calcd}, g cm^{-3}	1.602
μ(Mo Kα), cm^{-1}	36.21
S	1.07
cryst size, mm^3	0.28 × 0.38 × 0.58
$2\theta_{max}$, deg	51.1
T, K	296
no. of reflns measd	9817
no. of reflns obsd ($I \geq 3.0\sigma(I)$)	4641
R^a (%)	2.98
$R_w{}^b$ (%)	4.13

[a] $R = [\sum||F_o| - |F_c||/\sum|F_o|]$. [b] $R_w = [\sum w(||F_o| - |F_c||)^2/\sum w(|F_o|)^2]^{1/2}$; $w = A/(\sigma^2 F_o + BF_o{}^2)$.

Table 2. Selected Bond Distances (Å) and Angles (deg) for $[Tl(tpp)(OSO_2CF_3)(THF)\cdot THF]$ (**1**)

Distances			
Tl(1)−O(1)	2.387(6)	Tl(1)−N(1)	2.137(8)
Tl(1)−O(4)	2.778(7)	Tl(1)−N(2)	2.140(7)
O(1)−S(1)	1.455(8)	Tl(1)−N(3)	2.150(8)
O(2)−S(1)	1.42(1)	Tl(1)−N(4)	2.153(6)
O(3)−S(1)	1.416(9)	C(45)−F(1)	1.31(2)
S(1)−C(45)	1.77(2)	C(45)−F(2)	1.32(3)
		C(45)−F(3)	1.38(2)

Angles			
Tl(1)−O(1)−S(1)	129.6(5)	S(1)−C(45)−F(1)	113(1)
O(1)−S(1)−O(2)	113.8(5)	S(1)−C(45)−F(2)	112(1)
O(1)−S(1)−O(3)	116.0(5)	S(1)−C(45)−F(3)	108(2)
O(1)−S(1)−C(45)	100.7(8)	F(1)−C(45)−F(2)	109(2)
O(2)−S(1)−C(45)	105.2(8)	F(1)−C(45)−F(3)	108(1)
O(3)−S(1)−C(45)	104.1(7)	F(2)−C(45)−F(3)	107(1)
O(2)−S(1)−O(3)	114.7(7)	N(1)−Tl(1)−N(2)	89.2(3)
O(4)−Tl(1)−N(1)	83.0(3)	N(1)−Tl(1)−N(3)	164.6(2)
O(4)−Tl(1)−N(2)	78.6(2)	N(1)−Tl(1)−N(4)	88.2(3)
O(4)−Tl(1)−N(3)	81.7(3)	N(2)−Tl(1)−N(3)	89.2(3)
O(4)−Tl(1)−N(4)	87.5(2)	N(2)−Tl(1)−N(4)	166.1(2)
O(1)−Tl(1)−N(1)	97.2(3)	N(3)−Tl(1)−N(4)	89.7(3)
O(1)−Tl(1)−N(2)	95.0(2)	O(1)−Tl(1)−O(4)	173.6(3)
O(1)−Tl(1)−N(3)	98.2(3)	Tl(1)−O(4)−C(46)	124(1)
O(1)−Tl(1)−N(4)	98.9(2)	Tl(1)−O(4)−C(49)	124.7(8)

It is an octahedral complex of the porphyrin N_4, one triflate oxygen, and one THF oxygen. Bond distances are Tl(1)−O(1) = 2.387(6) Å, Tl(1)−O(4) = 2.778(7) Å, and the mean Tl(1)−N = 2.145(7) Å. The angle between the two axial oxygen ligands is nearly linear with O(1)−Tl(1)−O(4) = 173.6(3)°. The thallium−O(4) distance of 2.778(7) Å is long, but just within the sum of van der Waals radii of thallium and oxygen, ~3.5 Å. This longer Tl···O(4) contact is described as the effective coordination (or as "semicoordinated").[6,7] The short Tl(1)−O(1) distance and the displacement of the thallium atom toward the triflate are consistent with a much stronger metal ligand bond to the triflate anion than to the THF molecule. This type of asymmetry in bond lengths was also observed for $Fe(tpp)(OTeF_5)(THF)$ with $Fe-O(OTeF_5)$ = 1.967 Å and Fe−O(THF) = 2.334 Å.[8] In compound **1**, the interaction of $CF_3SO_3{}^-$ with thallium is purely unidentate, the second (or the third) triflate oxygen i.e. O(2) [or O(3)] being 3.592 (or 4.594 Å) from the thallium atom. The triflate is monodentate both in **1** and in $Si(tptp)(OSO_2CF_3)_2$.[2]

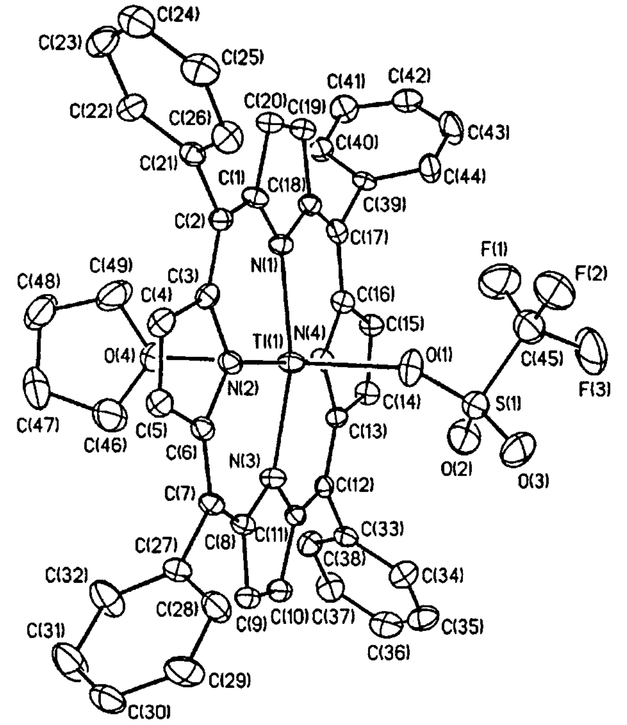

Figure 1. Molecular configuration and atom labeling scheme for $Tl(tpp)(OSO_2CF_3)(THF)\cdot THF$ (**1**). Hydrogen atoms and the free THF (or noncoordinated THF) are omitted for clarity.

The displacements of the metal center from the planes of the macrocycle atoms ($C_{20}N_4$) and the four porphyrin nitrogens are labeled as Δ24 and Δ4N, respectively. The Tl atom is 0.295/0.273 (i.e. Δ24/Δ4N) out of the porphyrin or N_4 plane toward the triflate oxygen. The dihedral angles between the mean plane ($C_{20}N_4$) and the plane of the phenyl group are 69.4° [C(24)], 82.7° [C(30)], 104.2° [C(36)], and 100.3° [C(42)]. The radius of the central "hole" (C_t'···N, the distance from the geometrical center (C_t') of the mean plane of the 24-atom core to the porphyrinato-core N atoms) in **1** is 2.128 Å, which is larger than 2.01 Å as suggested by Collin and Hoard.[9] The thallium(III) is bonded in a highly expanded porphyrinato core ($C_{20}N_4$) and the porphyrin ($C_{20}N_4$ and Tl) can be viewed as a MOOP (metal out-of-plane) shape.[10] Figure 2 illustrates the displacement (in Å) of each atom of the porphyrin ($C_{20}N_4$ and Tl) from the porphyrin mean plane ($C_{20}N_4$).

In general, the coodination sphere of the Tl^{3+} ion for the thallium porphyrins is an approximate square-based pyramid in which the apical site is occupied either by a bidentate group for complexes $Tl(tpp)(O_2CCF_3)$, $Tl(tmpp)(C_6H_5CO_2)$, and Tl(por)(OAc), with por = tpp, tmpp (5,10,15,20-tetra(4-methoxyphenyl)porphyrinate), tpyp (5,10,15,20-tetra(4-pyridyl)porphyrinate), or by a monodentate group for complexes [Tl(por)X] with the axial ligand X = CN, Cl, CH_3 and por = tpp, tmpp, tpyp (Table 3). These thallium porphyrins generally show Δ24 of 0.74−1.06 Å. However, the compound **1** is a distorted octahedron with O(1) (of triflato) and O(4) (of THF) in the trans position. To coordinate the O(1) of triflate and semicoordinate

---

(6) Deacon, G. B.; Philips, R. J. *Coord. Chem. Rev.* **1980**, *33*, 227.
(7) Scheidt, W. R.; Lee, Y. J.; Geiger, D. K.; Taylor, K.; Hatano, K. *J. Am. Chem. Soc.* **1982**, *104*, 3367.
(8) Kellett, P. J.; Pawlik, M. J.; Taylor, L. F.; Thompson, R. G.; Levstik, M. A.; Anderson, O. P.; Strauss, S. H. *Inorg. Chem.* **1989**, *28*, 440.
(9) Collins, D. M.; Hoard, J. L. *J. Am. Chem. Soc.* **1970**, *92*, 3761.
(10) Prendergast, K.; Spiro, T. G. *J. Am. Chem. Soc.* **1992**, *114*, 3793.

Table 3. Stereochemical Parameters for Thallium(III) Porphyrin Complexes

compound	Δ24 (Å)	binding of axial ligand (found)	distortion ($C_{20}N_4$ and Tl)	core size $C_t'\cdots N$ (Å)
$Tl(tpp)(O_2CCF_3)$[12]	0.741	bidentate	domed	2.092
Tl(tpp)(OAc)[19,20]	0.842	bidentate	domed	–
Tl(tmpp)(OAc)[24]	0.808	bidentate	domed	2.084
Tl(tpyp)(OAc)[25,26]	0.858	bidentate	domed	–
$Tl(tmpp)(C_6H_5CO_2)$[27]	0.811	bidentate	domed	2.096
Tl(tpp)(CN)[28]	0.908 1.027	monodentate	domed	–
Tl(tmpp)(CN)[17]	0.86	monodentate	domed	2.085
Tl(tpyp)(CN)[29]	0.825 0.900	monodentate	domed	–
Tl(tpp)Cl[30]	0.737	–	domed	–
Tl(tmpp)Cl[17]	0.82	–	domed	2.095
Tl(tpyp)Cl[31]	0.826 0.85	–	domed	2.091
$Tl(tpp)CH_3$[30]	0.979	–	domed	–
$Tl(tpyp)CH_3$[32]	1.059 0.975	–	domed	–
$Tl(tpp)(OSO_2CF_3)(THF)\cdot THF$	0.295	monodentate	MOOP	2.128

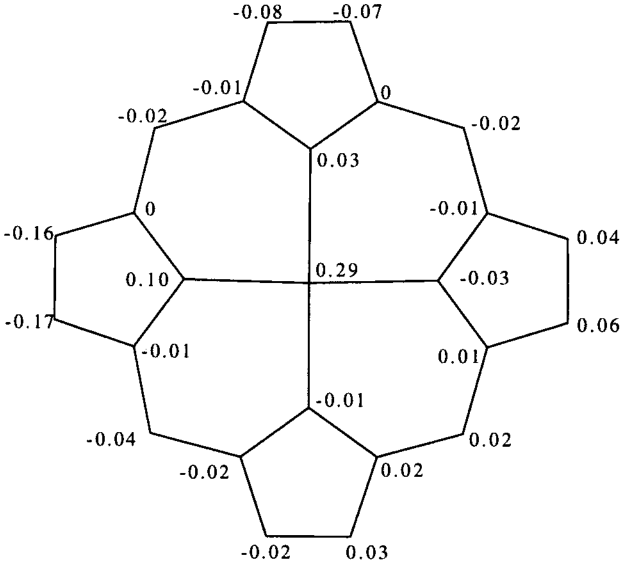

Figure 2. Diagram of the porphyrin core ($C_{20}N_4$ and Tl) of compound **1** showing the displacement (in Å) of the atoms from the mean plane of the porphyrin ($C_{20}N_4$).

the O(4) of THF simulataneously, the $T1^{3+}$ atom closely approaches the C_t' of $C_{20}N_4$, resulting in the smaller Δ24 of 0.295 Å for compound **1**. The displacement of the thallium atom depends at least partially on the relative importance of the binding of the two dissimilar axial ligands for the six-coordinate metal porphyrin complexes.[7] Some measurements are taken of the asymmetry in axial ligand binding with respect to the difference in axial bond lengths (Δ*l*). Interestingly, increasing Δ*l* from 0 (for the equivalent axial ligand, i.e. $[Fe(oep)(THF)_2]^+ClO_4^-)$[11] and 0.367 (for $Fe(tpp)(OTeF_5)(THF)$)[8] to 0.391 Å ($Tl(tpp)(OSO_2CF_3)(THF)$) causes an increase of the Δ24 from 0 and 0.20 to 0.295 Å.

^{13}C and ^{19}F for $Tl(tpp)(OSO_2CF_3)(THF)\cdot THF$ (1) in Acetone-d_6. Results obtained from the ^{13}C NMR studies of **1** in acetone-d_6 indicate that **1** ionizes completely and simply *via*

$$Tl(tpp)(OSO_2CF_3)(THF)\cdot THF \xrightarrow{\text{acetone-}d_6} Tl(tpp)^+ + CF_3SO_3^- + 2THF... \quad (1)$$

Table 4 summarizes ^{13}C data for **1** in acetone-d_6 at 24 and −80 °C. Eight major resonances with a α carbon (C_α) at $\delta = 149.8$, C_l at $\delta = 141.3$, $C_{2,6}$ at $\delta = 135.5$, C_β at $\delta = 134.1$, C_4 at $\delta = 129.2$, $C_{3,5}$ at $\delta = 127.9$, *meso* carbon (C_m) at $\delta = 122.7$ and the CF_3SO_3 carbon at $\delta = 121.2$ ppm were observed at −80 °C. Figure 3 shows the ^{13}C spectrum for **1** in acetone-d_6 at −100 °C. The ^{13}C resonance of CF_3SO_3 for compound **1**, as obtained by averaging over 24 and −80 °C at $\delta = 121.5 \pm 0.3$ ppm with ^1J(C−F) coupling constant 321 Hz, resembles that of ionic $CF_3SO_3^-$ (or free $CF_3SO_3^-$) with $\delta = 120.8 \pm 0.2$ and ^1J(C−F) = 322 Hz at room temperature (Table 4). ^{19}F NMR spectroscopy was used to examine the binding of $CF_3SO_3^-$ to $Tl(tpp)^+$. The fluorine resonance for $[Bu_4N^+][CF_3SO_3^-]$ in chloroform is found at −78.7 ppm (where $CFCl_3$ is used as an external reference) at room temperature.[4] The ^{19}F signal for compound **1** at 24 °C is −78.7 ppm (in THF-d_8) or −78.1 ppm (in acetone-d_6) resembles that in ionic $CF_3SO_3^-$. Both ^{13}C and ^{19}F data indicate that only the free $CF_3SO_3^-$ is detected for **1** in acetone-d_6. Although **1** is a THF solvate, disssolution in acetone-d_6 could produce $Tl(tpp)(THF)_2^+$, or the acetone adduct $Tl(tpp)(THF)(OC(CD_3)_2)^+$. However, when **1** is dissolved in acetone-d_6, the NMR resonances of THF downfield from Me_4Si are observed with similar chemical shifts at 67.7 and 25.9 ppm for ^{13}C at −100 °C (Figure 3a), at 67.9 and 26.3 ppm for ^{13}C at 24 °C, and at 3.59 and 1.77 ppm for ^1H at −100 and 24 °C. These resonances confirm that all THF is free THF. In addition, these data do not support the exchange between a small amount of coordinated THF and free THF for **1** in acetone-d_6. Meanwhile, the ^{13}C and ^1H NMR resonances of acetone downfield from TMS for **1** in acetone-d_6 at −100 and 24 °C are observed with the same chemical shifts at 206.2 and 29.8 ppm for ^{13}C (Figure 3a) and at 2.04 ppm for ^1H, respectively. These latter resonances indicate that all the acetone-d_6 is free deuterated acetone. Notably, all THF and acetone-d_6 are free when **1** is dissolved in acetone-d_6, implying that the cationic thallium species $Tl(tpp)^+$ is four-coordinate. The results above support the proposed dissociation of compound **1** in acetone-d_6 as shown in eq 1.

Solid-State CP/MAS ^{13}C and MAS ^{19}F for Compound (1). Table 4 presents the solid-state ^{13}C CP/MAS data of compound **1** at 24 °C. Five major resonances with C_α at $\delta = 150.5$, C_1 at 141.2, $C_{2,6}$ and C_β at $\delta = 133.5$, C_4 and $C_{3,5}$ at 128.6, and C_m and CF_3SO_3 at 121.2−122.7 ppm were observed. Due to the overlap of CF_3SO_3 with C_m, the unambiguous assignment of the carbon chemical shift for a coordinated triflate is impossible. However, the ^{19}F chemical shifts of the triflate ions are detected

---

(11) Masuda, H.; Taga, T.; Osaki, K.; Sugimoto, H.; Yoshida, Z.; Ogoshi, H. *Bull. Chem. Soc. Jpn.* **1982**, *55*, 3891.

Table 4. ^{19}F and ^{13}C Chemical Shifts (δ) and Tl−^{13}C Coupling Constant (J in Hz) for Tl(tpp)(OSO$_2$CF$_3$)(THF)·THF (**1**) in Acetone-d_6[a]

compound	solvent (carbon freq.)	T (°C)	C$_\alpha$	C$_1$	C$_{2,6}$	C$_\beta$	C$_4$	C$_{3,5}$	C$_m$	CF$_3$SO$_3$	^{19}F
Tl(tpp)(OSO$_2$CF$_3$)(THF)·THF (**1**)	acetone-d_6	24	150.5	141.9	135.5; 135.4	133.7	129.2	127.9	123.2	121.7	−78.1
	(100.61 MHz)		(7)	(19)		(170)			(166)	(320)[b]	−78.7[c]
	acetone-d_6	−80	149.8	141.3	135.5	134.1	129.2	127.9	122.7	121.2	−78.4
	(150.89 MHz)					(179)			(166)	(321)[b]	
(1)	solid	24	150.5	141.2	133.5		128.6		122.7−121.1		−74.0[d]
	(50.33 MHz)								(m)		
CF$_3$SO$_3^-$Na$^+$	DMSO-d_6	room temp	–	–	–	–	–	–	–	120.6[33]	–
										(322)	
Bu$_4$N$^+$CF$_3$SO$_3^-$	CDCl$_3$	room temp	–	–	–	–	–	–	–	121.0[33]	−78.7[4]
										(321)	

[a] Chemical shifts in ppm relative to the methyl carbon of acetone-d_6 at δ = 29.8. Values in parentheses beneath are J(Tl−^{13}C) coupling constants in Hz unless specified. ^{19}F was measured at 282.40 MHz unless specified. [b] ^1J(C−F) coupling constant. [c] It was measured in THF-d_8. [d] Solid-state ^{19}F was measured at 470.6 MHz.

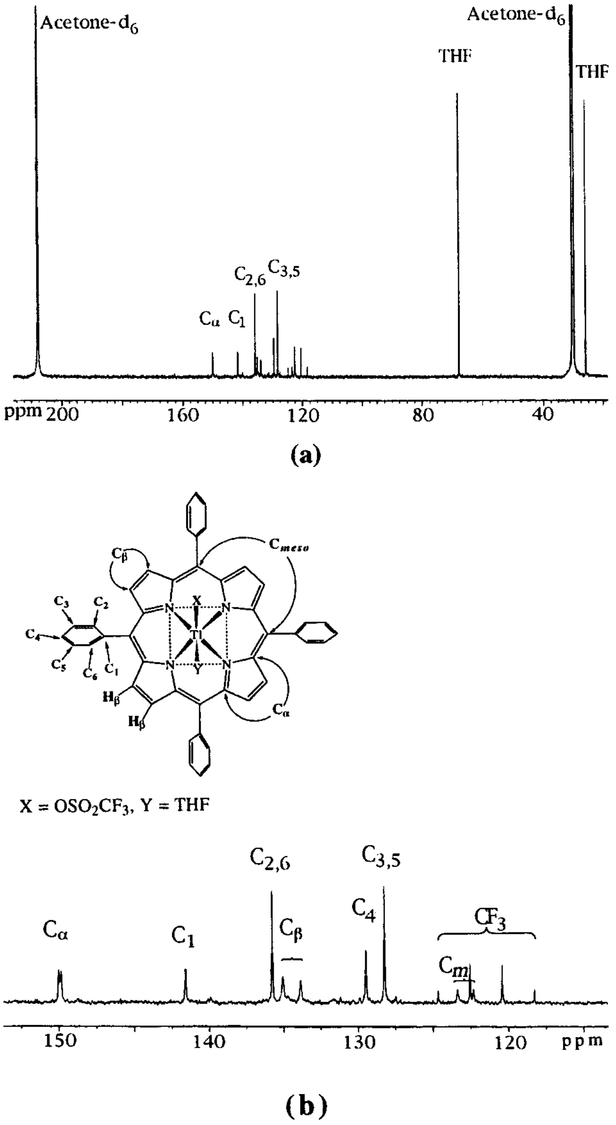

Figure 3. ^{13}C broad band NMR spectra for Tl(tpp)(OSO$_2$CF$_3$)(THF)·THF (**1**) in acetone-d_6 (150.92 MHz) at −100 °C: (a) entire spectrum; (b) expansion the region of 115−155 ppm in (a). TMS is used as internal reference.

when they are coordinated by the solid state ^{19}F NMR measurement. The resonance of the solid ^{19}F of compound **1** occurs as a broad singlet (line width 1700 Hz, ~3.6 ppm) at −74.0 ppm at 24 °C, which is ~4.7 ppm downfield of the fluorine resonance for [Bu$_4$N$^+$][CF$_3$SO$_3^-$]. Moreover, we cannot resolve the long-range coupling of ^{19}F to thallium, with a typical ^4J(Tl−F) value of ~29.2 ± 0.6 Hz,[12] for a coordinated triflate. This is despite the fact that the CF$_3$ group in **1** lies within the shielding region of **1**, which normally leads to upfield shifts. However, the downfield shift of ~4.7 ppm for F in the solid-state NMR is due to the shift of ^{19}F in **1** being controlled by the paramagnetic term,[13−16] not by the ring current effect. This paramagnetic contribution is a shift toward the lower field, which is the largest for covalent bonds of CF$_3$SO$_3$ in **1**. Our earlier work observed a similar downfield shift of ~3 ppm [from −78.07 (obtained from CF$_3$COOH) to −75.09 ppm] for ^{19}F in a 0.02 M solution of Tl(tmpp)(O$_2$CCF$_3$) in CD$_2$Cl$_2$ at −70 °C.[12]

UV/Visible Absorption Spectra for Compound 1. The electronic spectrum of **1** in acetone (or THF) and the cisoid six-coordinate thallium porphyrin complexes (e.g. Tl(tpp)(O$_2$CCF$_3$) and Tl(tpp)(OAc)) closely resemble with electronic absorption at 430 (B(0,0)), 564 (Q(1,0)), and 604 (Q (0,0)) for **1** versus 432, 566, and 606 nm for Tl(tpp)(O$_2$CCF$_3$)[12,17] and 433, 567, and 607 nm for Tl(tpp)(OAc).[18−20] This finding is due to the former spectrum being the spectrum of Tl(tpp)$^+$. Notably, the four-coordinate Tl(tpp)$^+$ and the cisoid six-coordinate thallium porphyrin complexes belongs to regular (or "normal") metalloporphyrins containing closed-shell Tl^{3+} ions (d^{10}), in which the d$_\pi$ (d$_{xz}$, d$_{yz}$) metal-based orbitals are relatively low in energy.[21,22] These low-energy orbitals only slightly influence the porphyrin π-to-π* energy gap in porphyrin electronic spectra. In contrast to most transition metal complexes, their color is due to absorption within the porphyrin ligand involving the excitation of electrons from π-to-π* porphyrin ring orbitals. When Tl binds to the porphyrin in Tl(tpp)$^+$ or in cisoid six-coordinate thallium porphyrin complexes, the absorption spectrum changes due to symmetric effects. However, the π-to-π* energy gap is negligibly affected

---

(12) Chou, L. F.; Chen, J. H. *J. Chem. Soc., Dalton Trans.* **1996**, 3787.
(13) Carrington, A.; McLachlan, A. D. *Introduction to Magnetic Resonance*; Harper and Row: New York, 1967; p 57.
(14) Pople, J. A.; Schneider, W. G.; Bernstein, H. J. *High-Resolution Nuclear Magnetic Resonance*; McGraw-Hill: New York, 1959; p 172.
(15) Eaton, D. R. In *Physical Methods in Advanced Inorganic Chemistry*; Hill, H. A. O., Day, H. Ed.; Wiley: New York, 1967; p 472.
(16) Yoder, C. H.; Schaeffer, C. D. *Introduction to Multinuclear NMR*; Benjamin/Cummings: Reading, MA, 1987; p 85.
(17) Senge, M. O.; Senge, K. R.; Regli, K. J.; Smith, K. M. *J. Chem. Soc., Dalton Trans.* **1993**, 3519.
(18) Abraham, R. J.; Barnett, G. H.; Smith, K. M. *J. Chem. Soc., Perkin Trans. 1* **1973**, 2142.
(19) Chen, J. C.; Jang, H. S.; Chen, J. H.; Hwang, L. P. *Polyhedron* **1991**, *10*, 2069.
(20) Suen, S. C.; Lee, W. B.; Hong, F. E.; Jong, T. T.; Chen, J. H.; Hwang, L. P. *Polyhedron* **1992**, *11*, 3025.
(21) Gouterman, M. In *The Porphyrins*; Dolphin, D., Ed.; Academic: New York, 1978; Vol. 3, Chapter 1.
(22) Marsh, D. F.; Mink, L. M. *J. Chem. Educ.* **1996**, *73*, 1188.

and a regular metallorporphyrin spectrum results. This phenomenon accounts for why variations of the axial ligand in Tl(tpp)$^+$ or in cisoid six-coordinate thallium complexes do not significantly affect the electronic spectra, although minor change are apparent.[18]

Conclusions

This investigation synthesizes and characterizes a new thallium(III) porphyrin complex Tl(tpp)(OSO_2CF_3)(THF)·THF (**1**). Metathesis reaction of Tl(tpp)Cl with Ag(CF_3SO_3) in THF solvent provides the convenient route to Tl(tpp)(OSO_2-CF_3)(THF):

$$\mathrm{Tl(tpp)Cl} + \mathrm{Ag(CF_3SO_3)} \xrightarrow{\mathrm{THF}} \mathrm{AgCl_{(s)}} + \mathrm{Tl(tpp)(OSO_2CF_3)(THF)}... \quad (2)$$

Tl(tpp)(OSO_2CF_3)(THF) is formed by eq 2 and dissociates by eq 1. This compound has little or no stability outside the crystal lattice; its existence is directly attributed to the solid-state lattice effects.[23]

The typical thallium(III) porphyrin is cisoid five- or six-coordinate with a large thallium atom displacement (0.74−1.06 Å) from a modestly domed porphyrinato core (with an average $C_t'\cdots N$ of 2.091 Å). The complex **1** studied herein is the first structurally characterized transoid six-coordinate thallium(III) porphyrin complex with the thallium atom locating (0.295 Å) slightly out of the plane toward $OSO_2CF_3^-$ and having a radially expanded core (with an average $C_t'\cdots N$ of 2.128 Å). ^{1}H, ^{13}C, and ^{19}F of the triflate and THF for compound **1** in acetone-d_6 (THF-d_8) at −80 and 24 °C confirm that complex **1** ionizes completely to Tl(tpp)$^+$ and ionic $CF_3SO_3^-$ in acetone-d_6 (or THF-d_8).

Acknowledgment. Financial support from the National Research Council of the R.O.C. under Grant NSC 87-2113-M-005-001 is gratefully acknowledged.

Supporting Information Available: Tables of structure determination summary, atomic coordinates, bond lengths, bond angles, anisotropic displacement, and H-atom coordinates coefficients and ORTEP diagrams for compound **1** (14 pages). An X-ray crystallographic file, in CIF format, for compound **1** is also available on the Internet only. Ordering and access information is given on any current masthead page.

IC9803199

---

(23) Scheidt, W. R.; Mondal, J. U.; Eigenbrot, C. W.; Adler, A.; Radonovich, L. J.; Hoard, J. L. *Inorg. Chem.* **1986**, *25*, 795.

(24) Sheu, Y. H.; Hong, T. N.; Lin, C. C.; Chen, J. H.; Wang, S. S. *Polyhedron* **1997**, *16*, 681.

(25) Fuh, J. J.; Tang, S. S.; Lin, Y. H.; Chen, J. H.; Liu, T. S.; Wang, S. S.; Lin, J. C. *Polyhedron* **1994**, *13*, 3031.

(26) Tang, S. S.; Lin, Y. H.; Sheu, M. T.; Lin, C. C.; Chen, J. H.; Wang, S. S. *Polyhedron* **1995**, *14*, 1241.

(27) Sheu, Y. H.; Hong, T. N.; Chen, J. H.; Liao, F. L.; Wang, S. L.; Wang, S. S.; Yang, T. C. *Polyhedron* **1997**, *16*, 1621.

(28) Lee, W. B.; Suen, S. C.; Jong, T. T.; Hong, F. E.; Chen, J. H.; Lin, H. J.; Hwang, L. P. *J. Organomet. Chem.* **1993**, *450*, 63.

(29) Cheng, T. W.; Chen, Y. J.; Hong, F. E.; Chen, J. H.; Hwang, L. P. *Polyhedron* **1994**, *13*, 403.

(30) Henrick, K.; Matthews, R. W.; Tasker, P. A. *Inorg. Chem.* **1977**, *16*, 3293.

(31) Tang, S. S.; Liu, I. C.; Lin, C. C.; Chen, J. H.; Wang, S. S. *Polyhedron* **1996**, *15*, 37.

(32) Tang, S. S.; Sheu, M. T.; Lin, Y. H.; Liu, I. C.; Chen, J. H.; Wang, S. S. *Polyhedron* **1995**, *14*, 301.

(33) Pouchert, C. J.; Behnke, J. *The Aldrich Library of ^{13}C and ^{1}H FT NMR Spectra*, 1st ed.; Aldrich: Milwaukee, WI, 1993; Vol. 1, P1431-(A, B).